The syntheses and X-ray crystal structures of novel transition metal cluster arrays containing 2–5 coordinated $[(CO)_9Co_3(\mu_3\text{-}CCOO)]^-$ ligands in a variety of geometries

Victor Calvo-Perez[a], Maoyu Shang[a], Glenn P.A. Yap[b], Arnold L. Rheingold[b], Thomas P. Fehlner[a,*]

[a]*Departments of Chemistry and Biochemistry, University of Notre Dame, Notre Dame IN 46556, USA*
[b]*University of Delaware, Newark, DE 19716, USA*

Abstract

Reaction of $(CO)_9Co_3(\mu_3\text{-}CCOOH)$ with metal trifluoroacetates leads to the isolation of $Cr_2\{\mu\text{-}OOC\text{-}CCo_3(CO)_9\}_2\{\mu\text{-}OOCCF_3\}_2(THF)_2$, **1**, and $Sm_2\{\mu\text{-}OOCCCo_3(CO)_9\}_2\{\mu\text{-}OOCCF_3\}_4\{(CO)_9Co_3CCOOH\}_2(THF)_2\cdot 2THF$, **2**, which are cluster substituted analogs of known organic carboxylates. Reaction of Pt(II) acetate, prepared in situ, with $(CO)_9Co_3(\mu_3\text{-}CCOOH)$ leads to $PtCo\{\mu\text{-}OOCCCo_3(CO)_9\}_3(\mu\text{-}OOCCH_3)\{(CO)_9Co_3CCOOH\}$, **3**, which contains an unusual Pt(II)Co(II) dimeric core. Reaction of $Zn(OH)_2$ with $(CO)_9Co_3(\mu_3\text{-}CCOOH)$ in THF leads to $Zn_4(\mu_4\text{-}O)\{\mu\text{-}OOC\text{-}CCo_3(CO)_9\}_6$ but in 2-MeTHF the reaction leads to $ZnCo\{\mu\text{-}OOC\text{-}CCo_3(CO)_9\}_3\{Co(CO)_4\}\{2\text{-}(CH_3)C_4H_7O\}$, **4**. This compound features the presence of a $[Co(CO)_4]^-$ moiety coordinated to a Co(II) center. Reaction of Cr(II) acetate with $(CO)_9Co_3(\mu_3\text{-}CCOOH)$ in noncoordinating solvents results in $CoCr_2(\mu_3\text{-}O)\{\mu\text{-}OOC\text{-}CCo_3(CO)_9\}_4(\mu\text{-}OOCCH_3)_2\{(CO)_9Co_3CCOOH\}_2(H_2O)\cdot C_7H_8$, **5a**, and $Cr_3(\mu_3\text{-}O)\{\mu\text{-}OOCCCo_3(CO)_9\}_4(\mu\text{-}OOCCH_3)_2\{(CO)_9Co_3C\text{-}COOH\}(CH_3OOH)_2\cdot C_7H_8$, **5b**, which are cluster ligand analogs of known organic carboxylate oxo metal trimers. Finally, deprotonation of $(CO)_9Co_3(\mu_3\text{-}CCOOH)$ with a bulky base inhibits the base degradation of the tricobalt cluster sufficiently such that $[C_{10}H_6(N(CH_3)_2)_2H][Co_2\{\mu\text{-}OOCCCo_3(CO)_9\}_3\{OOCCCo_3(CO)_9\}_2]$, **6**, can be isolated. All compounds are structurally characterized by X-ray crystallography and selected spectroscopic techniques.

Keywords: Cobalt; Chromium; Zinc; Platinum; Samarium; Clusters; Carboxylates

1. Introduction

There has been considerable interest in recent years in the logical synthesis of large molecular systems. The approaches utilized to date are varied and lead, for example, to one-dimensional chains [1] or rings [2] or two-dimensional sheets [3] or three-dimensional dendritic moieties [4]. Both organic reactions as well as coordination reactions have been employed to yield an impressive variety of new substances with interesting properties. We have explored a related area namely the synthesis of transition metal cluster arrays using the concept of a functionalized cluster as a ligand towards a cationic metal center [5]. While our compounds derive from monofunctional clusters, others have used bifunctional clusters to form linear cluster arrays [6,7]. Our work has also illustrated some of the differences a typical metal cluster, e.g. $(CO)_9Co_3(\mu_3\text{-}C\text{-})$, imparts to the coordinating ability of the ligand functionality, e.g. $-COO^-$, towards various cationic metal centers [8]. In addition, some of the compounds have found use as precursors to novel heterogeneous hydrogenation catalysts [9–11].

As the cluster acid, $(CO)_9Co_3(\mu_3\text{-}CCOOH)$, degrades under basic conditions, the synthetic challenge has been to find ways to convert the acid to the $[(CO)_9Co_3(\mu_3\text{-}CCO_2)]^-$ coordinated ligand without decomposing the cobalt cluster into organic and inorganic fragments. Some of these compounds have been studied in detail and we have provided efficient routes for gram scale syntheses [5,8,12–20]. As described herein, other approaches have now been explored and have uncovered an additional set of new compounds with varied cluster ligand coordination numbers as well as unusual cationic cores. The result is a set of cluster arrays that mimic most of the classical geometries of coordination chemistry and provide some unique spatial arrays as well. In the following we describe

*Corresponding author. Tel.: +1-219-631-7058; fax: +1-219-631-6652.
E-mail address: Thomas.P.Fehlner.1@nd.edu (T.P. Fehlner)

the preparation and structures of these new cluster metal carboxylates.

2. Experimental

2.1. Syntheses

Anhydrous $CrCl_2$, CF_3COOH, $Na[CF_3COO]$, $Ag[CH_3COO]$, and $PtBr_2$ were purchased form Aldrich and used as received. Proton sponge® $C_{10}H_6(N(CH_3)_2)_2$ (Aldrich) was sublimed under vacuum at 30°C on a Schlenk line. Samarium metal (American Potash and Chem. Corp, 99.9%) was dissolved in aqueous CF_3COOH (50%) and after 1 week, the clear solution was slowly evaporated to yield white crystals of $Sm(OOCCF_3)_3(H_2O)_2$. $Zn(OH)_2$ gel was prepared from 4.4 g $Zn(CH_3COO)_2{\cdot}2H_2O$ (Aldrich) aqueous solution and diluted ammonia and the mixture was brought to pH 8.0. The gel, thus obtained was centrifuged three times with deionized water and later washed thoroughly on a column with deionized water until no further base was released. 2-Methyl-tetrahydrofuran was purchased from Aldrich and distilled over Na before use. $(CO)_9Co_3(\mu_3\text{-}CCOOH)$ was prepared as described previously [21]. $Cr_2(OOCCF_3)_4{\cdot}(OEt_2)_2$ was prepared as described in the literature [22]. All the solvents used were distilled under nitrogen just before use. All reactions were performed under Ar on a Schlenk line using standard methods. IR: Nicolet 205 FTIR. UV–Vis: Perkin-Elmer Model 6 or 19 spectrophotometers. MS: JEOL JMS-AX 505HA mass spectrometer in FAB mode. NMR: GN 300 MHz spectrometer. EPR: Brucker 1600 EPR spectrometer working in the X-band and equipped with an Oxford variable temperature controller. XPS: Kratos SAM 800 spectrometer with a magnesium anode using C1s at 285.0 eV as reference.

2.1.1. $Cr_2\{\mu\text{-}OOC\text{-}CCo_3(CO)_9\}_2\{\mu\text{-}OOCCF_3\}_2(THF)_2$, 1

A 400 mg (0.57 mmol) amount of $Cr_2(OOCCF_3)_4{\cdot}(OEt_2)_2$ plus 80 mg (0.59 mmol) CF_3COONa and 300 mg (0.62 mmol) of $(CO)_9Co_3(\mu_3\text{-}CCOOH)$ in 10 ml THF plus 20 ml toluene afforded a deep purple–blue solution. Stirring under argon at 30°C for 45 min gave a black–brown solution. The solvents were removed under vacuum and the black solid was dispersed in 30 ml freshly distilled toluene with sonication. The extract was quickly filtered on a fine frit funnel to remove the solids. The filtrate was left at room temperature for 1 day in the dark and then moved to 4°C for a week. Crystalline **1** in 32% yield (260 mg, 0.18 mmol) based on Cr was isolated. IR (KBr, cm^{-1}): 2988 (w), 2866 (w), 2110 (w), 2055 (vs), 2040 (sh), 1986 (m), 1659 (m), 1499 (w), 1473 (w), 1388 (m), 1343 (w), 1203 (m), 1160 (m), 1080 (w), 1041 (w), 822 (w), 852 (w), 792 (w), 757 (m), 728 (m), 558 (m), 529 (m), 504 (m), 422 (w). UV–Vis (toluene, nm, $M^{-1}cm^{-1}$): 380 sh, 516 (ε 2,600). Analysis (dried under vacuum). Found, C 24.38%, F 7.80%, Co 24.14%, Cr 7.17%. Calculated for $C_{26}Co_6Cr_2F_6O_{26}$: C 26.26%, F 8.31%, Co 25.57%, Cr 7.58%.

2.1.2. $Sm_2\{\mu\text{-}OOCCCo_3(CO)_9\}_2\{\mu\text{-}OOCCF_3\}_4\{(CO)_9Co_3CCOOH\}_2(THF)_2{\cdot}2THF$, 2

To 0.120 g (0.228 mmol) of solid $Sm(OOCCF_3)_3(H_2O)_2$ dispersed in 10 ml THF was added a solution of 0.500 g (1.029 mmol) of $(CO)_9Co_3(\mu_3\text{-}CCOOH)$ in 20 ml THF. After mixing at 30°C for 1 h, the solvent was removed under vacuum. The solid was extracted with hot toluene, filtered, kept at 10°C for 1 day, and then at −20°C. Well formed crystals of **2** were isolated in 88% yield based on samarium (0.310 g, 0.104 mmol). Recrystallization produced X-ray quality crystals. IR (KBr, cm^{-1}): 2113 (w), 2051 (s), 1707 (m), 1607 (m), 1479 (w), 1488 (w), 1365 (w), 1339 (w), 1264 (w), 1205 (m), 1153 (w), 797 (w), 781 (w), 720 (w), 544 (w), 500 (w). EPR (X-band) powder, g: 2.17, Δp–p: 55 G.

2.1.3. $PtCo\{\mu\text{-}OOCCCo_3(CO)_9\}_3(\mu\text{-}OOCCH_3)\{(CO)_9Co_3CCOOH\}$, 3

Reaction of $PtBr_2$ and 2 $AgOOCCH_3$ in water followed by removal of the AgBr by filtration yielded a brown–yellow solid after removal of the solvent. Presumably this is the simple acetate as IR spectra showed that it is not $Pt_4(OOCCH_3)_8$. The latter compound, prepared separately using the closely related method of Yamaguchi et al. [23], yielded only Pt metal on reaction with the cluster acid. A solution of 0.40 g of the fresh Pt intermediate was combined with 1.31 g (2.70 mmol) of $(CO)_9Co_3(\mu_3\text{-}CCOOH)$ in 100 ml THF and the mixture was stirred in the dark at 45°C for 4 days. After filtration, the THF was removed under vacuum and the solid extracted with 70 ml toluene. The volume of the solution was reduced to 25 ml at 60°C and slowly cooled to 10°C at which temperature it was kept for 2 weeks. Crystalline **3** (0.20 g, 0.09 mmol) was isolated. IR (KBr, cm^{-1}) 2946 (w), 2110 (m), 2047 (vs), 1642 (w), 1625 (sh), 1584 (w), 1355 (m), 1328 (m), 1279 (w), 1069 (w), 768 (w), 722 (m), 546 (w), 527 (m), 499 (m), 462 (w). MS (negFAB, NBA, Xe) m/z 2250.1 (10%); calculated m/z 2254. Analysis. Found: C 25.18%, H<0.5%, Co 34.3%, Pt 7.70%. Calculated for $C_{46}H_4Co_{13}PtO_{46}$: C 24.52%, H 0.18%, Co 33.99%, Pt 8.66% .

2.1.4. $ZnCo\{\mu\text{-}OOCCCo_3(CO)_9\}_3\{Co(CO)_4\}\{2\text{-}(CH_3)C_4H_7O\}$, 4

A 58 mg amount of $Zn(OH)_2$ gel (0.090 mmol of Zn) with 1.00 g (2.06 mmol) of $(CO)_9Co_3CCOOH$ dissolved in 15 ml THF' (=2-$(CH_3)C_4H_7O$) was stirred for 30 m at room temperature (RT) and the black–brown mixture was then sonicated for 15 min to further disperse the gel. The solvents were removed at 37°C under vacuum and the dark–brown solid was dispersed in 35 ml freshly distilled

toluene plus 1 ml THF' yielding a brown solution and a dark-brown precipitate. The brown solution was filtered and the filtrate stood at room temperature for one day and then −20°C for a week. Crystals of **4** were obtained in 73% yield based on Zn (120 mg, 0.066 mmol) by layering with hexane. Note that the use of THF leads to the production of $Zn_4(m_4\text{-}O)\{\mu\text{-}OOC\text{-}CCo_3(CO)_9\}_6$ [5] in 70% yield. IR (KBr cm^{-1}): 2960 (w), 2110 (m), 2055–2045 (vs), 1974 (s), 1963 (s), 1944 (s), 1565 (m), 1496 (w), 1379 (s), 1340 (m), 1085 (w), 793 (w), 751 (m), 722 (m), 556 (m), 530 (m), 528 (m), 499 (m), 473 (w). ^1H NMR (CD_2Cl_2, d, 20°): 8.3 br m, 6.5 br s, 3.4 br s, 2.6 br s, 1.2 br s. UV–Vis (CH_2Cl_2, nm, $M^{-1}cm^{-1}$): 300 (ε 13,300), 524 (ε 2,300). XPS confirms the existence of Zn ($2p^{3/2}$, 1021 and $2p^{1/2}$, 1044 eV) and Co ($2p^{3/2}$, 780 and $2p^{1/2}$, 795 eV) in the ratio of ≈1:9. Analysis (dried under vacuum). Found, Co 41.47%, Zn 4.21% (10.98 Co/Zn mol ratio). Calculated for $C_{37}Co_{11}ZnO_{37}$: Co 37.04%, Zn 3.74% (11.0 Co/Zn mol ratio).

2.1.5. $CoCr_2(\mu_3\text{-}O)\{\mu\text{-}OOCCCo_3(CO)_9\}_4(\mu\text{-}OOCCH_3)_2\{(CO)_9Co_3CCOOH\}_2(H_2O)\cdot C_7H_8$, **5a**

0.443 g (1.18 mmol) of $Cr_2(OOCCH_3)_4(H_2O)_2$, synthesized by published methods [24], were dispersed with sonication in 30 ml of CH_2Cl_2 in a two-neck Schlenk flask and mixed with 2.983 g (6.14 mmol) of $(CO)_9Co_3C$-COOH dissolved in 20 ml CH_2Cl_2 under Ar. The solution was sonicated three times for 5 min and allowed to react at 35°C for 24 h. The solvent was removed under vacuum at room temperature and the residue extracted with two 25 ml portions of toluene, and filtered cold. The yield of crystalline product was 40% (730 mg 0.22 mmol) based on Cr. IR (KBr pellet, cm^{-1}) 2962 (w), 2929 (w), 2109 (w), 2056 (s), 2045 (s), 2038 (s), 1694 (w), 1636 (w), 1600 (w), 1560 (w), 1379 (m), 1330 (m), 1263 (w), 1084 (w), 757 (w), 730 (w), 722 (w), 556 (w), 529 (w), 501 (m), 418 (w). UV–Vis (CH_2Cl_2, nm, $M^{-1}cm^{-1}$) 512 (ε 9,030), 380(sh), 302 (ε 75,000). EPR(crystals, X-band) silent at room temperature. Analysis: Found: C 28.72%, H 0.77%, Co 32.08%. Calculated for $C_{77}H_{18}Co_{19}Cr_2O_{72}$: C 27.87%, H 0.55%, Co 33.74%. MS (negFAB, Xe, NBA CH_2Cl_2) Found: *m/z* 1997.0 (22%), 2133.8 *m/z* (15%), 2156.5 *m/z* (25%). Calculated: *m/z* 1997.0 $Co(C_{11}Co_3O_{11})_4$, *m/z* 2133.8 $C_{48}H_6^{52}Cr_2Co_{12}O_{48}$ -CO, *m/z* 2156.5 $C_{48}H_6^{52}Cr_2Co_{12}O_{48}$ -4H.

2.1.6. $Cr_3(\mu_3\text{-}O)\{\mu\text{-}OOCCCo_3(CO)_9\}_4(\mu\text{-}OOCCH_3)_2\{(CO)_9Co_3CCOOH\}(CH_3OOH)_2\cdot C_7H_8$, **5b**

The same reaction mixture as for **5a** gave a small yield (50 mg, 0.02 mmol) of a second compound. IR (KBr pellet, cm^{-1}) 2963 (w), 2932 (w), 2111 (w), 2043 (s), 1645 (w), 1562 (w-br), 1430 (w), 1386 (w), 1252 (w), 1080 (w), 760 (w), 722 (m), 697 (w), 554 (m), 527 (m), 500(s), 418 (w). EPR (X-band) powder, g: 2.01, Δp–p: 500 G, single crystal, g: 1.98, Δp–p: 520 G.

2.1.7. $[C_{10}H_6(N(CH_3)_2)_2H][Co_2\{\mu\text{-}OOCCCo_3(CO)_9\}_3\{OOCCCo_3(CO)_9\}_2]$, **6**

A 45-mg (0.093 mmol) amount of $(CO)_9Co_3CCOOH$ were placed in a Schlenk tube together with 20 mg (0.093 mmol) of proton sponge® $C_{10}H_6(N(CH_3)_2)_2$ and 2 ml of CH_2Cl_2. After reaction for 2 h at 45°C the warm solution was filtered and layered with 4 ml of toluene and left standing at room temperature for 5 days. Nicely shaped black crystals (22 mg, 0.0079 mmol), suitable for X-ray slowly grew from this solution. IR: (KBr pellet, cm^{-1}): 2109(m), 2040 (s), 1580 (m), 1541 (m), 1382 (m), 1338 (m), 749 (m), 723 (m), 551 (m), 528 (m), 501 (m), 408 (m). (CH_2Cl_2, cm^{-1}): 2108 (w), 2068 (s), 2040 (s), 1579 (w), 1542 (w), 1383 (m). UV–Vis (CH_2Cl_2, nm, $M^{-1}cm^{-1}$): 520 (ε 5,500), 350 sh. Magnetic susceptibility (Evans method, CD_2Cl_2, 20°) $c=7.08\times10^{-3}$ $cm^{-3}mol^{-1}$. EPR (powder, 4 K) g: 2.04, Δp–p: 116 G, and a sharp signal at g: 2.13, Δp–p: 2300 G. Analysis: Found C 29.86%, H 0.83%, N 1.11%. Calculated for $C_{69}H_{19}Co_{17}N_2O_{55}$ C 30.05%, H 0.69%, N 1.02%.

2.2. Structure determinations

2.2.1. $Cr_2\{\mu\text{-}OOC\text{-}CCo_3(CO)_9\}_2\{\mu\text{-}OOCCF_3\}_2(THF)_2$, **1**

Crystals of **1** suitable for X-ray diffraction were grown from a saturated solution of **1** in toluene kept at 10°C for a month. Crystal data and experimental details are given in Table 1. A block-like black crystal with dimensions 0.58×0.32×0.22 mm was mounted in a glass capillary in a random orientation and data were collected with an Enraf–Nonius CAD4 diffractometer equipped with a graphite crystal monochromated Mo Kα X-radiation source. The structure was solved by the MULTAN direct methods followed by successive different Fourier syntheses. Full-matrix least-squares refinements were employed. All-non-hydrogen atoms were refined with anisotropic thermal parameters in the final cycles. $R=0.04085$, $R_w=0.05394$, (370 variables refined) for 2642 reflections with $F_o^2 > 3\sigma(F_o^2)$.

2.2.2. $Sm_2\{\mu\text{-}OOCCCo_3(CO)_9\}_2\{\mu\text{-}OOCCF_3\}_4\{(CO)_9Co_3CCOOH\}_2(THF)_2\cdot 2THF$, **2**

A black plate-like crystal was mounted on a glass fiber with its long axis roughly parallel to the Phi axis of the goniometer. Data were collected with an Enraf–Nonius CAD4 diffractometer equipped with a graphite crystal monochromated Mo Kα X-radiation source. Crystal data and experimental details are given in Table 1. The structure was solved by direct methods. A total of seven metal atoms were located from an E-map and the remaining were located in succeeding difference Fourier syntheses. Hydrogen atoms were not included in the calculations. The structure was refined in full-matrix least-squares. All-non-hydrogen atoms were refined with anisotropic thermal parameters in the final cycles. $R_1=0.04531$,

Table 1
Crystal data for compounds **1–6**

	1	**2**	**3**	**4**	**5a**	**5b**	**6**
Formula	$C_{34}H_{18}Co_6Cr_2F_6O_{28}$	$C_{68}H_{34}Co_{12}Sm_2F_{12}O_{56}$	$C_{46}H_4Co_{13}PtO_{46}$	$C_{45}Co_{11}ZnO_{58}$	$C_{77}H_{18}Co_{19}Cr_2O_{72}$	$C_{70}H_{27}Co_{15}Cr_3O_{64}$	$C_{69}H_{19}Co_{13}N_2O_{55}$
F.W.	1444.07	2982.87	2253.74	1862.0	3318.68	2927.91	2757.67
$F(000)$	1416	1446	4308		3234	5728	10768
Crystal dimensions	0.58×0.32×0.22 mm	0.13×0.18×0.48 mm	0.55×0.28×0.12 mm	0.42×0.44×0.56 mm	0.18×0.09×0.14 mm	0.55×0.36×0.35 mm	0.40×0.40×0.40 mm
Mo Kα radiation	λ=0.71073 Å	λ=0.71073 Å	λ=0.71073 Å	λ=0.71073 Å	λ=0.71073 Å	λ=0.71073 Å	λ=0.71073 Å
Temperature	20°C	20°C	20°C	20°C	20°C	20°C	−27°C
Space group	$P2_1/n$	Pi	$P2_1/c$	$P2_1/n$	Pi (No. 2)	$P2_1/n$ (No. 14)	$P2_1/c$
a	10.662(1)A	13.6311(9) Å	21.759(4) Å	12.222(5)	14.500 (3) Å	17.770 (5) Å	26.069(7) Å
b	12.430(3) Å	13.952(2) Å	17.979(3) Å	22.584 (6)	20.291 (4) Å	21.367 (2) Å	24.439 (5) Å
c	19.415(3) Å	16.691(2) Å	20.053(5) Å	24.052 (6)	20.817 (3) Å	28.075 (7) Å	30.236 (13) Å
α		104.23(1)°			71.60 (1)°		
β	94.76(1)°	101.096(7)°	114.91(2)°	92.35	80.90 (1)°	102.69 (1)°	90.70 (3)°
γ		115.638(9)°			80.26 (2)°		
V	2564.1(8) Å^3	2606.7(6) Å^3	7115(3) Å^3	6633 (20)	5692 (2) Å^3	10400 (4) Å^3	19261 (11) Å^3
Z	2	1	4	4	2	4	8
Cal. density	1.870 g/cm^3	1.900 g/cm^3	2.104 g/cm^3	1.865 g/cm^3	1.936 g/cm^3	1.870 g/cm^3	1.902 g/cm^3
μ(Mo Kα)	23.916 cm^{-1}	30.751 cm^{-1}	50.180 cm^{-1}	29.637 cm^{-1}	29.637 cm^{-1}	27.117 cm^{-1}	29.41 cm^{-1}
No. of reflections measured	4260 total, 3434 unique	7573 total, 7216 unique	10447 total, 8781 unique	9398 total, 9081 unique	10556 total, 10556 unique	14948 total, 11088 unique	21148 total, 20645 unique
Corrections	Lorentz-polarization	Lorentz-polarization	Lorentz-polarization		Lorentz-polarization	Lorentz-polarization	
	Linear decay (from 0.999 to 1.294 on I)	Linear decay (from 0.985 to 1.131 on I)	Linear decay (from 0.981 to 1.306 on I)		Linear decay (from 0.998 to 1.183 on I)	Linear decay (from 1.000 to 1.157 on I)	
	Reflection averaging (agreement on I=1.6%)	Reflection averaging (agreement on I=2.5%)	Reflection averaging (agreement on I=3.1%)		Empirical absorption (from 0.89 to 1.00 on I)	Reflection averaging (agreement on I=2.2%)	
	Empirical absorption (0.8250–0.9977 on I)	Empirical absorption (0.6516–0.9998 on I)	Empirical absorption (0.5978–0.9990 on I)			Empirical absorption (from 0.9269 to 0.9998 on I)	
Solution	Direct methods	Direct methods	Direct methods	Direct methods	Direct methods	Direct methods	Direct methods
hydrogen atoms	Not included	Not included	Not included	Not included	Not included	Not located	Idealized
Refinement	Full-matrix least-squares	Full-matrix least-squares	Full-matrix least-squares	Full-matrix least-squares	Full-matrix least-squares	Full-matrix least-squares	Full-matrix least-squares
Minimization function	$\Sigma w(\|F_o\|-\|F_c\|)^2$	$\Sigma w(\|F_o\|-\|F_c\|)^2$	$\Sigma w(\|F_o\|-\|F_c\|)^2$	$\Sigma w(\|F_o\|-\|F_c\|)^2$	$\Sigma w(\|F_o\|-\|F_c\|)^2$	$\Sigma w(\|F_o\|-\|F_c\|)^2$	$\Sigma w(\|F_o\|-\|F_c\|)^2$
Least-squares weights	$4F_o^2/\sigma^2(F_o^2)=1/\sigma^2(F_o)$	$4F_o^2/\sigma^2(F_o^2)=1/\sigma^2(F_o)$	$4F_o^2/\sigma^2(F_o^2)=1/\sigma^2(F_o)$	$4F_o^2/\sigma^2(F_o^2)=1/\sigma^2(F_o)$	$4F_o^2/\sigma^2(F_o^2)=1/\sigma^2(F_o)$	$4F_o^2/\sigma^2(F_o^2)=1/\sigma^2(F_o)$	$4F_o^2/\sigma^2(F_o^2)=1/\sigma^2(F_o)$
Anomalous dispersion	All non-hydrogen atoms	All non-hydrogen atoms	All non-hydrogen atoms	All non-hydrogen atoms	All non-hydrogen atoms	All non-hydrogen atoms	All non-hydrogen atoms
Reflections included	2642 with $F_o^2>3.0\sigma(F_o^2)$	5781 with $F_o^2>3.0\sigma(F_o^2)$	7226 with $F_o^2>3.0\sigma(F_o^2)$	3910 with $F_o2>3.0\sigma(F_o^2)$	6422 with $F_o^2>3.0\sigma(F_o^2)$	6507 with $F_o^2>3.0\sigma(F_o^2)$	20638 with $F_o^2>4.0\sigma(F_o^2)$
Parameters refined	370	663	955		787	930	1315
Unweighted agreement factor	0.04085	0.04531	0.03683	0.0705	0.070	0.08231	0.1260
Weighted agreement factor	0.05 394	0.06065	0.04770	0.0737	0.085	0.1074	0.2783
Esd of obs. of unit weight	1.824	2.077	1.536		2.26	2.240	
Convergence, largest shift	0.02	0.03	0.01		0.26	0.03	
High peak in final diff. map	0.70(7) e/Å^3	0.92 (11) e/Å^3	1.56(10) e/Å^3	0.97 e/Å^3	2.38(13) e/Å^3	1.13(13) e/Å^3	4.178 e/Å^3
Low peak in final diff. map	−0.32(7) e/Å^3	−0.86(11) e/Å^3	−0.64(10) e/Å^3		−0.85(13) e/Å^3	−0.85(13) e/Å^3	−1.863 e/Å^3

$R_1=\Sigma|F_o-F_c|/\Sigma|F_o|$, $R_2=(\Sigma w(F_o-F_c)^2/\Sigma wF_o^2)^{1/2}$.

Table 2
Selected bond distances and angles for **1**

	Bond	Distance [Å]		Angle		Angle [°]
Cr	Cr	2.427(1)	Cr	O(2)	C(1)	121.4(3)
Cr	O(1)	1.993(4)	Cr	O(3)	C(3)	117.7(3)
Cr	O(2)	2.002(4)	Cr	O(4)	C(3)	118.5(3)
Cr	O(3)	2.028(4)	O(1)	C(1)	0(2)	123.6(5)
Cr	O(4)	2.021(4)	O(1)	C(1)	C(2)	118.1(4)
Cr	O(5)	2.234(4)	O(2)	C(1)	C(2)	118.3(4)
Co(1)	Co(2)	2.456(1)	O(1)	Cr	0O(2)	174.2(1)
Co(1)	Co(3)	2.449(1)	O(1)	Cr	O(3)	90.9(1)
Co(1)	C(2)	1.884(5)	O(1)	Cr	O(4)	88.6(1)
Co(1)	C(11)	1.780(6)	O(1)	Cr	O(5)	94.2(1)
Co(1)	C(12)	1.825(8)	O(2)	Cr	O(3)	89.2(1)
Co(1)	C(13)	1.748(8)	O(2)	Cr	O(4)	90.8(1)
Co(2)	Co(3)	2.458(1)	O(2)	Cr	O(5)	91.6(1)
			O(3)	Cr	O(4)	174.8(1)
			O(3)	Cr	O(5)	92.0(1)
			0O4)	Cr	O(5)	93.2(1)

R_2=0.06065, (663 variables refined) for 5781 reflections with $F_o^2 > 3\sigma(F_o^2)$.

2.2.3. $PtCo\{\mu\text{-}OOCCCo_3(CO)_9\}_3(\mu\text{-}OOCCH_3)\{(CO)_9Co_3CCOOH\}$, 3

A black plate-like crystal was mounted in a glass capillary in a random orientation and data were collected

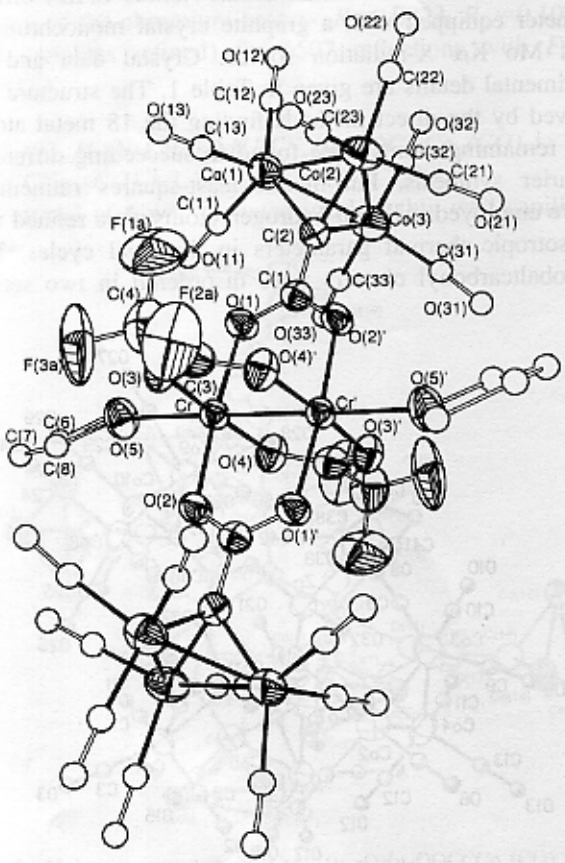

Fig. 1. Molecular structure of $Cr_2\{\mu\text{-}OOC\text{-}CCo_3(CO)_9\}_2\{\mu\text{-}OOCCF_3\}_2(THF)_2$, **1**.

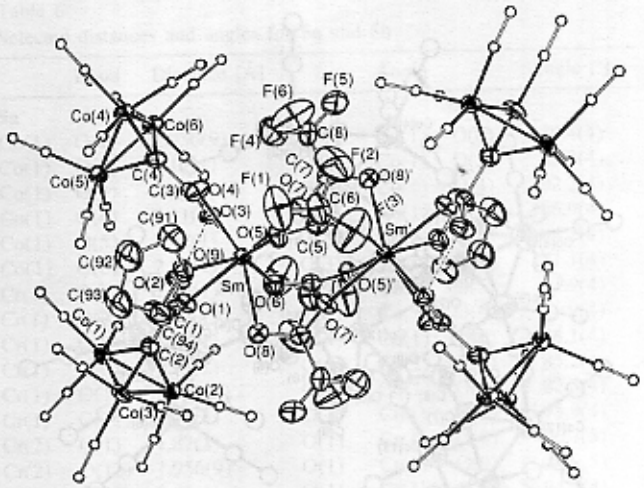

Fig. 2. Molecular structure of $Sm_2\{\mu\text{-}OOCCCo_3(CO)_9\}_2\{\mu\text{-}OOCCF_3\}_4\{(CO)_9Co_3CCOOH\}_2(THF)_2\cdot 2THF$, **2**.

with an Enraf–Nonius CAD4 diffractometer equipped with a graphite crystal monochromated Mo Kα X-radiation source. Crystal data and experimental details are given in Table 1. The structure was solved by direct methods followed by successive different Fourier syntheses. Full-matrix least-squares refinements were employed. All-non-hydrogen atoms were refined with anisotropic thermal parameters in the final cycles. R_1=0.03683, R_2=0.04770, (955 variables refined) for 7226 reflections with $F_o^2 > 3\sigma(F_o^2)$.

2.2.4. $ZnCo\{\mu\text{-}OOCCCo_3(CO)_9\}_3\{Co(CO)_4\}\{2\text{-}(CH_3)C_4H_7O\}$, 4

A suitable crystal of **3** was mounted in a thin wall capillary under nitrogen. Crystal data and experimental details are given in Table 1. The unit cell parameters were obtained by the least-squares refinement of the angular settings of 24 reflections ($20° \le 2\theta \le 24°$). Approximately 10% of the data was rejected by the learnt-profile routine

Table 3
Selected bond distances and angles for **2**

	Bond	Distance [Å]		Angle		Angle [°]
Sm	O(1)	2.475(5)	O(1)	Sm	O(3)	71.8(1)
Sm	O(3)	2.483(5)	O(1)	Sm	O(4)	97.1(2)
Sm	O(4)	2.420(5)	O(1)	Sm	O(5)	144.8(1)
Sm	O(5)	2.410(6)	O(1)	Sm	O(6)	73.3(2)
Sm	O(6)	2.39(5)	O(1)	Sm	O(7)	141.5(2)
Sm	O(7)	2.379(4)	O(1)	Sm	O(8)	74.1(2)
Sm	O(8)	2.462(5)	O(1)	Sm	O(9)	74.4(2)
Sm	O(9)	2.467(5)	O(3)	Sm	O(4)	53.0(2)
			O(3)	Sm	O(5)	134.3(1)
			O(6)	Sm	O(7)	75.1(2)
			O(6)	Sm	O(8)	79.9(2)
			O(6)	Sm	O(9)	143.9(2)
			O(7)	Sm	O(8)	120.8(2)
			O(7)	Sm	O(9)	140.8(2)
			O(8)	Sm	O(9)	76.0(2)
			O(5)	Sm	O(9)	73.8(2)

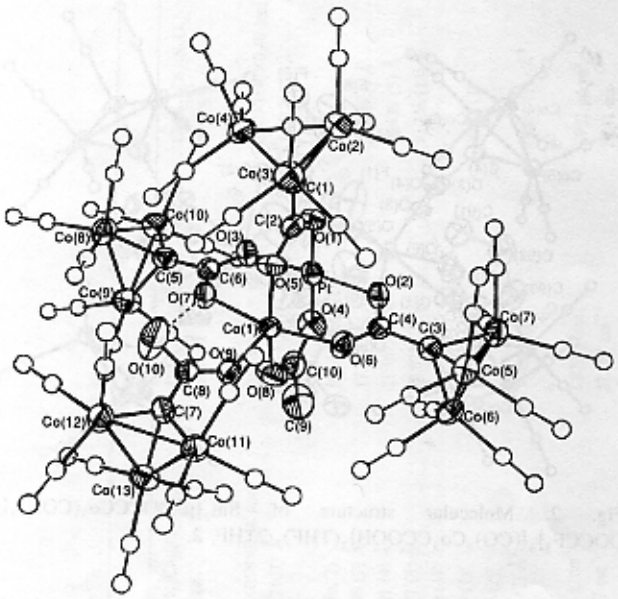

Fig. 3. Molecular structure of $PtCo\{\mu\text{-}OOCCCo_3(CO)_9\}_3(\mu\text{-}OOCCH_3)\{(CO)_9Co_3CCOOH\}$, **3**.

as contributions from a minor twin or satellite crystal. The unit cell of this compound contains four dimers, where two are structurally different clusters. The structure was solved by direct methods and completed by subsequent difference Fourier synthesis and refined by full-matrix least-squares procedures. Carbon atoms were refined isotropically. A Me-THF molecule coordinated to the Zn appears to be thermally disordered. A benzene molecule was found near an inversion center with an occupancy of 50% and was refined as a rigid body. Hydrogen atoms were ignored. The remaining peak in the difference map (0.97 e/Å^3) occurs at a chemically unreasonable position and was considered as noise.

2.2.5. $CoCr_2(\mu_3\text{-}O)\{\mu\text{-}OOCCCo_3(CO)_9\}_4(\mu\text{-}OOCCH_3)_2\{(CO)_9Co_3CCOOH\}_2(2H_2O).C_7H_8$, **5a**

Crystals of **5a** suitable for X-ray diffraction were grown from a warm toluene extract of **5a** left at room temperature for a week. A black plate-like crystal was mounted on a glass fiber with its long axis parallel to the phi axis of the goniometer. Data were collected with an Enraf–Nonius CAD4 diffractometer equipped with a graphite crystal monochromatic and Mo Kα X-radiation source. Crystal data and experimental details are given in Table 1. The structure was solved by direct methods where we found 21 metal atoms and followed by successive different Fourier syntheses. Full-matrix least-squares refinements were employed. All-non-hydrogen atoms were refined with anisotropic thermal parameters in the final cycles. Two toluene molecules were found in two different sets of inversion centers. $R=0.070$, $R_w=0.085$, (787 variables refined) for 6422 reflections with $F_o^2>3\sigma(F_o^2)$.

Table 4
Selected bond distances and angles for **3**

	Bond	Distance [Å]		Angle		Angle [°]
Pt	Co(1)	2.506(1)	O(1)	Pt	O(2)	90.0(2)
Pt	O(1)	1.995(5)	O(1)	Pt	O(3)	91.9(2)
Pt	O(2)	2.006(4)	O(1)	Pt	O(4)	177.9(2)
Pt	O(3)	2.018(4)	O(2)	Pt	O(3)	178.1(2)
Pt	O(4)	1.996(6)	O(2)	Pt	O(4)	88.6(2)
Co(1)	O(5)	2.071(5)	O(3)	Pt	O(4)	89.6(2)
Co(1)	O(6)	2.036(4)	O(5)	Co(1)	O(6)	89.9(2)
Co(1)	O(7)	2.138(4)	O(5)	Co(1)	O(7)	85.7(2)
Co(1)	O(8)	2.049(6)	O(5)	Co(1)	O(8)	165.8(2)
Co(1)	O(9)	2.013(5)	O(5)	Co(1)	O(9)	95.3(2)
			O(6)	Co(1)	O(7)	164.9(2)
			O(6)	Co(1)	O(8)	91.8(2)
			O(6)	Co(1)	O(9)	100.5(2)
			O(7)	Co(1)	O(8)	89.1(2)
			O(7)	Co(1)	O(9)	94.3(2)
			O(8)	Co(1)	O(9)	98.3(2)

2.2.6. $Cr_3(\mu_3\text{-}O)\{\mu\text{-}OOCCCo_3(CO)_9\}_4(\mu\text{-}OOCCH_3)_2\{(CO)_9Co_3CCOOH\}(CH_3OOH)_2\cdot C_7H_8$, **5b**

Crystals of **5b** suitable for X-ray diffraction were grown from a hot saturated extract of **5b** in toluene left at room temperature for one day and cooled to 10°C for a week. A black crystal was mounted on a glass capillary with its long axis parallel to the phi axis of the goniometer and data were collected with an Enraf–Nonius CAD4 diffractometer equipped with a graphite crystal monochromator and Mo Kα X-radiation source. Crystal data and experimental details are given in Table 1. The structure was solved by the direct methods finding the 18 metal atoms, the remaining atoms were found in succeeding difference Fourier synthesis. Full-matrix least-squares refinements were employed. All-non-hydrogen atoms were refined with anisotropic thermal parameters in the final cycles. Two tricobaltcarbonyl clusters were disordered in two sets of

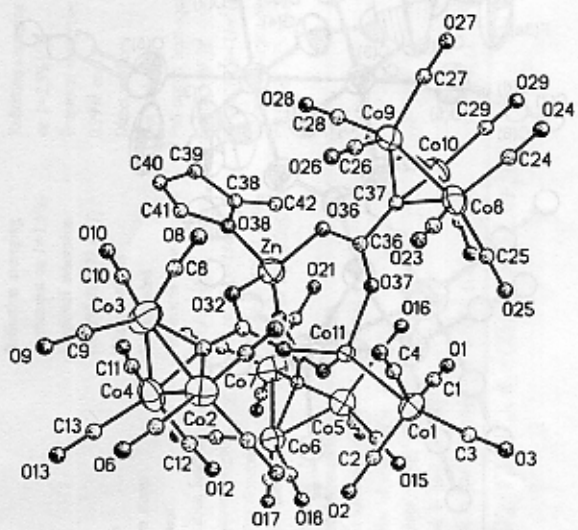

Fig. 4. Molecular structure of $ZnCo\{\mu\text{-}OOCCCo_3(CO)_9\}_3\{Co(CO)_4\}\{2\text{-}(CH_3)C_4H_7O\}$, **4**.

Table 5
Selected bond distances and angles for 4

Bond	Distance [Å]	Angle	Angle [Å]
Co(1)–Co(11)	2.419(4)		
Zn–O(32)	1.917(13)	Zn–O(32)–C(32)	126.7(12)
Zn–O(35)	1.921(12)	O(32)–Zn–O(35)	112.2(5)
		Zn–O(35)–C(34)	130.2(5)
Zn–O(36)	1.923(11)	O(32)–Zn–O(36)	112.5(12)
		Zn–O(36)–C(36)	122.8(12)
Zn–O(38)	1.982(13)	O(32)–Zn–O(38)	102.5(5)
Co(1)–C(1)	1.792(23)	Co(1 1)–Co(1)–C(1)	75.6(7)
Co(1)–C(2)	1.722(27)	Co(1 1)–Co(1)–C(3)	88.7(8)
Co(1)–C(3)	1.790(23)	Co(11)–Co(1)–C(3)	167.6(7)
Co(1)–C(4)	1.754(25)	Co(11)–Co(1)–C(4)	73.2(9)
Co(11)–O(33)	1.969(14)	Co(1)–Co(11)–O(33)	119.4(4)
		Co(11)–O(33)–C(32)	143.2(13)
Co(11)–O(34)	1.943(13)	Co(1)–Co(11)–O(34)	113.3(4)
		Co(11)–O(34)–C(34)	139.4(13)
Co(11)–O(37)	1.969(13)	Co(1)–Co(11)–O(37)	108.2(4)
		Co(11)–O(37)–C(36)	144.8(13)
Co(8)–Co(9)	2.455(4)		
Co(8)–Co(10)	2.4.64(4)	Co(8)–Co(9)–Co(10)	60.1(1)
Co(9)–Co(10)	2.466(4)	Co(9)–Co(8)–Co(10)	60.2(1)

positions with occupancies of 0.73 and 0.27, the rotational disorder about the C(3)–C(4) bond was successfully modeled. A toluene molecule was found with the methyl group disordered. The hydrogen atoms were not found but three H-bonded carboxylic acid show up in the terminal position of the chromium centers. $R=0.0823$, $R_w=0.1074$, (930 variables refined) for 6507 reflections with $F_o^2 > 3.0\sigma(F_o^2)$.

2.2.7. $[C_{10}H_6(N(CH_3)_2)_2H][Co_2\{\mu\text{-}OOCCCo_3(CO)_9\}_3\{OOCCCo_3(CO)_9\}_2]$. 6

A crystal of **6** was mounted inside a thin wall capillary

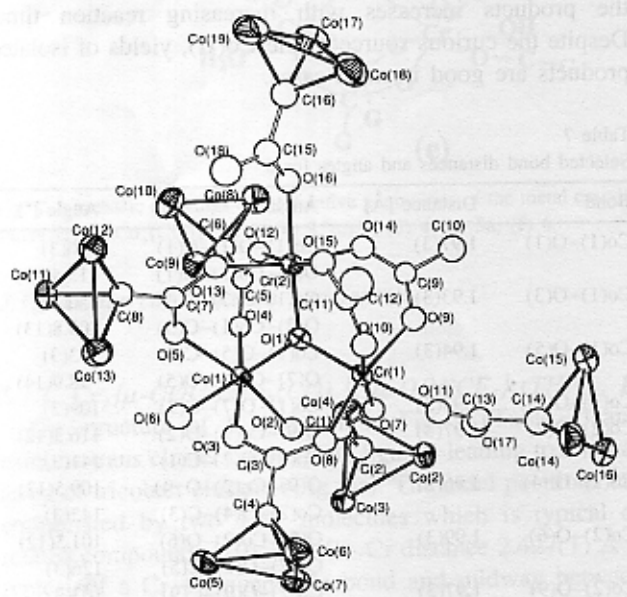

Fig. 5. Molecular structure of $CoCr_2(\mu_3\text{-}O)\{\mu\text{-}OOCCCo_3(CO)_9\}_4(\mu\text{-}OOCCH_3)_2\{(CO)_9Co_3CCOOH\}_2(H_2O)\cdot C_7H_8$, **5a**. The CO ligands have been removed from the tricobalt clusters for clarity.

Table 6
Selected distances and angles for **5a** and **5b**

	Bond	Distance [Å]		Angle		Angle [°]
5a						
Co(1)	O(1)	1.936(9)	O(1)	Co(1)	O(6)	179.4(4)
Co(1)	O(2)	2.12(1)	O(2)	Co(1)	O(3)	85.8(4)
Co(1)	O(3)	2.12(1)	O(2)	Co(1)	O(4)	92.2(4)
Co(1)	O(4)	2.11(1)	O(2)	Co(1)	O(5)	166.9(4)
Co(1)	O(5)	2.12(1)	O(2)	Co(1)	O(6)	84.2(4)
Co(1)	O(6)	2.13(1)	O(3)	Co(1)	O(4)	171.1(4)
Cr(1)	O(1)	1.85(1)	O(3)	Co(1)	O(5)	91.9(4)
Cr(1)	O(7)	2.020(9)	O(3)	Co(1)	O(6)	86.0(4)
Cr(1)	O(8)	1.96(1)	O(4)	Co(1)	O(5)	88.1(4)
Cr(1)	O(9)	1.99(1)	O(4)	Co(1)	O(6)	85.2(4)
Cr(1)	O(10)	1.957(9)	O(5)	Co(1)	O(6)	82.8(4)
Cr(1)	O(11)	2.10(1)	O(1)	Cr(1)	O(7)	95.9(4)
Cr(2)	O(1)	1.87(1)	O(1)	Cr(1)	O(8)	96.7(5)
Cr(2)	O(12)	1.956(9)	O(1)	Cr(1)	O(9)	94.9(5)
Cr(2)	O(13)	2.01(1)	O(1)	Cr(1)	O(10)	94.3(4)
Cr(2)	O(14)	1.96(1)	O(1)	Cr(1)	O(11)	175.6(5)
Cr(2)	O(15)	1.987(9)	O(7)	Cr(1)	O(8)	89.9(4)
Cr(2)	O(16)	2.09(1)	O(7)	Cr(1)	O(9)	85.6(4)
			O(7)	Cr(1)	O(10)	169.7(4)
			O(7)	Cr(1)	O(11)	86.9(4)
			O(8)	Cr(1)	O(9)	167.9(5)
			O(8)	Cr(1)	O(10)	90.1(4)
5b						
Cr(1)	O(1)	1.868(9)	O(1)	Cr(1)	O(2)	178.4(4)
Cr(1)	O(2)	2.10(1)	O(1)	Cr(1)	O(3)	96.8(4)
Cr(1)	O(3)	1.968(9)	O(1)	Cr(1)	O(4)	94.0(4)
Cr(1)	O(4)	1.99(1)	O(1)	Cr(1)	O(5)	96.6(4)
Cr(1)	O(5)	1.98(1)	O(1)	Cr(1)	O(6)	95.5(4)
Cr(1)	O(6)	2.021(9)	O(2)	Cr(1)	O(3)	81.8(4)
Cr(2)	O(1)	1.856(9)	O(2)	Cr(1)	O(4)	85.4(4)
Cr(2)	O(7)	2.10(1)	O(2)	Cr(1)	O(5)	84.0(4)
Cr(2)	O(8)	1.971(8)	O(2)	Cr(1)	O(6)	85.9(4)
Cr(2)	O(9)	2.01(1)	O(3)	Cr(1)	O(4)	91.7(4)
Cr(2)	O(10)	1.95(1)	O(3)	Cr(1)	O(5)	89.9(4)
Cr(2)	O(11)	2.008(9)	O(3)	Cr(1)	O(6)	167.7(4)
Cr(3)	O(1)	1.940(9)	O(4)	Cr(1)	O(5)	169.0(4)
Cr(3)	O(12)	2.16(1)	O(4)	Cr(1)	O(6)	86.6(4)
Cr(3)	O(13)	2.07(1)	O(5)	Cr(1)	O(6)	89.5(4)
Cr(3)	O(14)	2.06(1)	O(1)	Cr(2)	O(7)	177.6(4)
Cr(3)	O(15)	2.05(1)	O(1)	Cr(2)	O(8)	95.6(4)
Cr(3)	O(16)	2.05(1)	O(1)	Cr(2)	O(9)	93.4(4)
C(1)	O(3)	1.28(2)	O(1)	Cr(2)	O(10)	96.8(4)
C(1)	O(8)	1.23(2)	O(1)	Cr(2)	O(11)	95.5(4)
C(1)	C(2)	1.47(2)	O(7)	Cr(2)	O(8)	83.2(4)
C(3)	O(4)	1.24(2)	O(7)	Cr(2)	O(9)	84.6(4)
C(3)	O(9)	1.24(2)	O(7)	Cr(2)	O(10)	85.3(4)
			O(7)	Cr(2)	O(11)	85.6(4)
			O(8)	Cr(2)	O(9)	92.0(4)
			O(8)	Cr(2)	O(10)	90.4(4)
			O(8)	Cr(2)	O(11)	168.7(4)
			O(9)	Cr(2)	O(10)	169.3(4)
			O(9)	Cr(2)	O(11)	85.4(4)
			O(10)	Cr(2)	O(11)	90.3(4)
			O(1)	Cr(3)	O(12)	175.9(4)
			O(1)	Cr(3)	O(13)	97.7(4)
			O(1)	Cr(3)	O(14)	94.5(4)
			O(1)	Cr(3)	O(15)	93.7(4)
			O(1)	Cr(3)	O(16)	95.7(4)
			O(12)	Cr(3)	O(13)	85.5(4)
			O(12)	Cr(3)	O(14)	83.0(4)
			O(12)	Cr(3)	O(15)	88.8(4)
			O(12)	Cr(3)	O(16)	81.0(4)

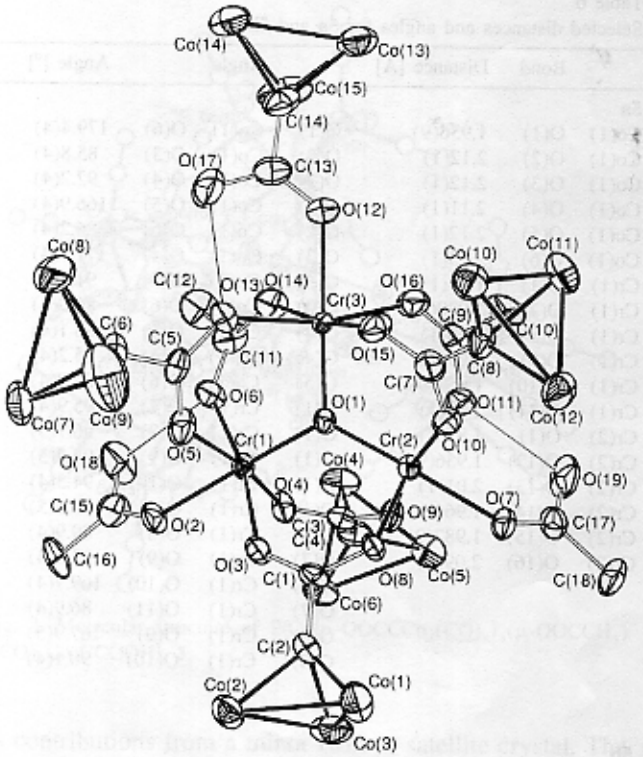

Fig. 6. Molecular structure of $Cr_3(\mu_3\text{-}O)\{\mu\text{-}OOCCCo_3(CO)_9\}_4(\mu\text{-}OOCCH_3)_2\{(CO)_9Co_3CCOOH\}(CH_3OOH)_2\cdot C_7H_8$, **5b**. The CO ligands have been removed from the tricobalt clusters for clarity.

under nitrogen. Crystal data and experimental details are given in Table 1. The unit cell parameters were obtained by the least-squares refinement of the angular settings of 24 reflections ($20° \leq 2\theta \leq 25°$). Systematic absences are uniquely consistent with space group $P2_1/c$. The structure was solved by direct methods and completed by subsequent difference Fourier synthesis and refined by full-matrix least-squares procedures. There are two independent but chemically equivalent cluster anions in the asymmetric unit. The remaining peak in the difference map (4.18 e/Å^3) occurs at a chemically unreasonable positions and were considered artifacts arising from less than satisfactory absorption coefficients. All crystals of **6** that were examined diffracted weakly and broadly indicating a large mosaic spread.

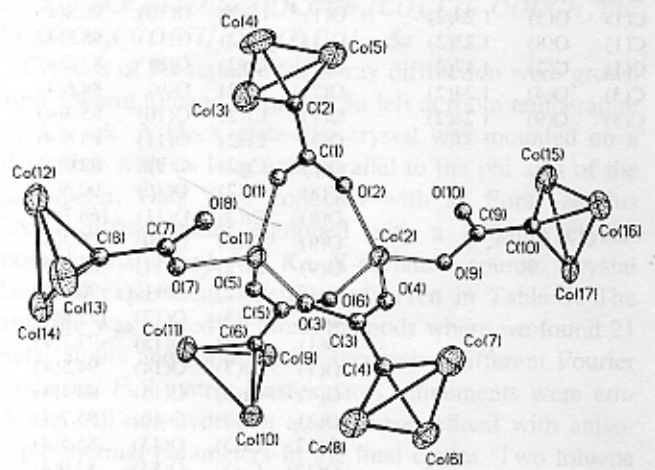

Fig. 7. Molecular structure of $[C_{10}H_6(N(CH_3)_2)_2H][Co_2\{\mu\text{-}OOCCCo_3(CO)_9\}_3\{OOCCCo_3(CO)_9\}_2]$, **6**. The CO ligands have been removed from the tricobalt clusters for clarity.

3. Results and discussion

Descriptions of the structures of the various cluster coordination compounds are presented below and salient features discussed proceeding from low to high cluster coordination number. In all cases, the structure of the tricobalt cluster in the ligand remains invariant within experimental error. Hence, the emphasis is on cluster coordination number, geometry, and core properties. Here the terms cluster coordination number and geometry refer only to the coordinated cluster ligands $[(CO)_9Co_3(\mu_3\text{-}COO)]^-$, i.e. our interest lies primarily in the spatial array of the tricobalt clusters rather than the complete coordination properties of the cationic metal cores which serve to support these arrays. Some compounds contain weakly coordinating cluster acid and this is ignored in defining the geometry of the cluster array. The coordinated cluster acid is known to be easily lost in solution [12]. Most likely it is found in the crystalline materials used for structural characterization as it fills some of the large voids that would exist in its absence, i.e., the tricobalt cluster substituent has substantial steric bulk.

Several of the new compounds contain Co(II) and one a $Co(CO)_4$ fragment. As discussed previously [5,14,21], these species arise from the degradation of the tricobalt cluster during reaction. The likelihood of finding them in the products increases with increasing reaction time. Despite the curious source of the Co(II), yields of isolated products are good in most cases.

Table 7
Selected bond distances and angles for **6**

Bond	Distance [Å]	Angle	Angle [°]
Co(1)–O(1)	1.97(3)	Co(1)–O(1)–C(1)	130(3)
		O(7)–Co(1)–O(1)	113.4(13)
Co(1)–O(3)	1.93(3)	Co(1)–O(3)–C(3)	130(3)
		O(7)–Co(1)–O(3)	109.8(13)
Co(1)–O(5)	1.94(3)	Co(1)–O(5)–C(5)	143(3)
		O(7)–Co(1)–O(5)	98.9(14)
Co(1)–O(7)	1.93(3)	Co(1)–O(7)–C(7)	109(3)
Co(2)–O(2)	1.97(3)	O(9)–Co(2)–O(2)	116.3(12)
		Co(2)–O(2)–C(1)	141(3)
Co(2)–O–4)	1.96(3)	O(9)–Co(2)–O–4)	109.5(12)
		Co(2)–O(4)–C(3)	142(3)
Co(2)–O(6)	1.99(3)	O(9)–Co(2)–O(6)	101.5(12)
		Co(2)–O(6)–C(5)	126(3)
Co(2)–O(9)	1.97(3)	Co(2)–O(9)–C(9)	103(3)
Co(3)–Co(4)	2.44(2)		
Co(3)–Co(5)	2.456(13)	Co(3)–Co(4)–Co(5)	60.5(4)
Co(4)–Co(5)	2.439(12)	Co(4)–Co(5)–Co(3)	59.7(5)

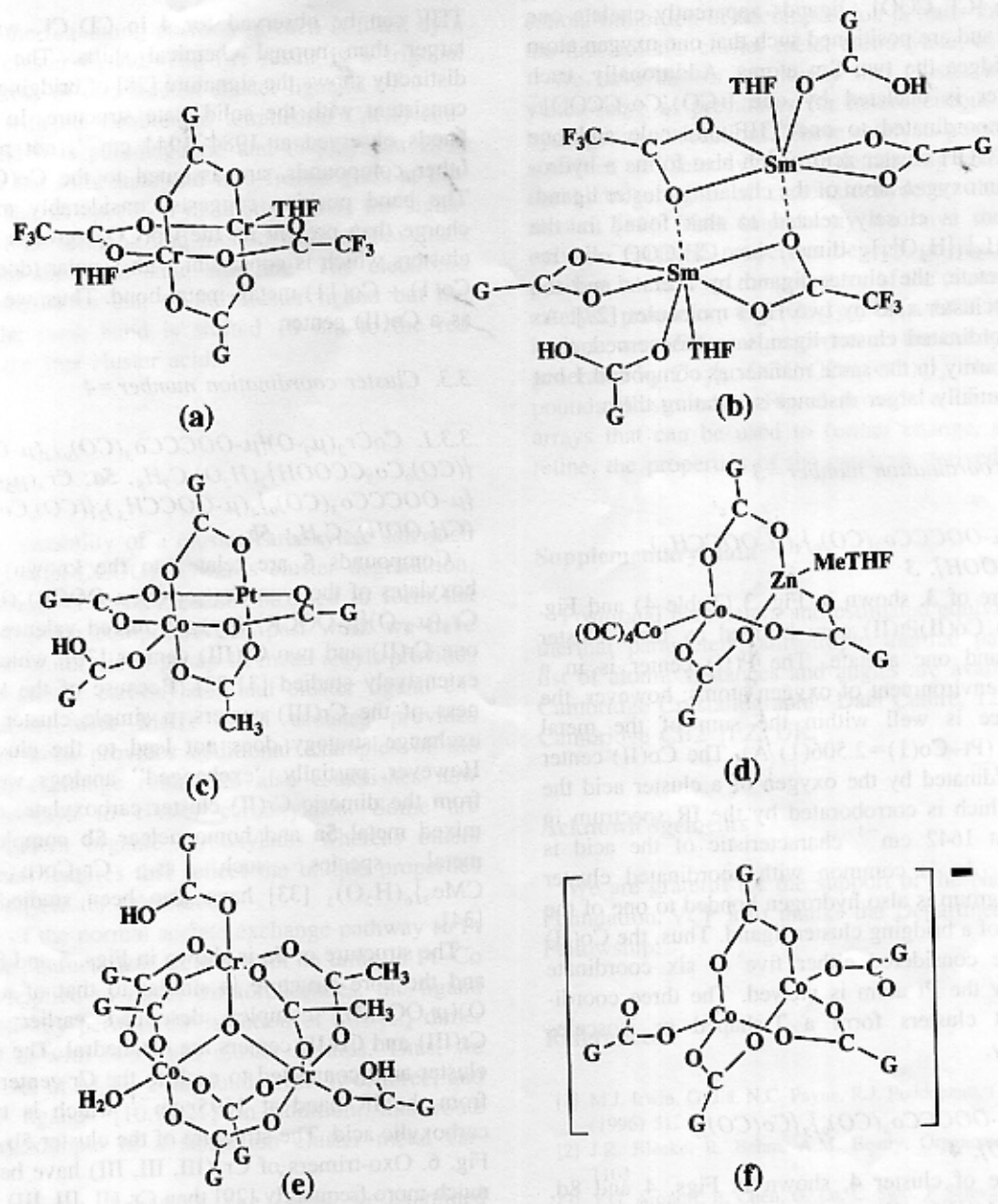

Fig. 8. Schematic drawings of the relative geometries of the metal coordinated cluster ligands for structurally characterized cluster coordination compounds where G=–$CCo_3(CO)_9$: (a) **1**, (b) **2**,*(c) **3**, (d) **4**, (e) **5a**, (f) **6**.

3.1. Cluster coordination number=2

3.1.1. $Cr_2\{\mu\text{-}OOC\text{-}CCo_3(CO)_9\}_2\{\mu\text{-}OOCCF_3\}_2(THF)_2$, **1**

The structure of **1** is shown in Fig. 1 (Table 2) and exhibits trans cluster carboxylate ligands leading to a linear array of tricobalt clusters (Fig. 8a). The axial positions are coordinated by two THF molecules which is typical of related compounds [10]. The Cr–Cr distance 2.427(1) Å is typical of a Cr–Cr quadruple bond and midway between that of $Cr_2(\mu\text{-}OOCCF_3)_4(THF)_2$ (2.541 Å) [25] and that of $Cr_2(\mu\text{-}OOCCH_3)_4(CH_3CCOOH)_2$ (2.300 Å) [26]. This suggests that the $[(CO)_9Co_3(\mu_3\text{-}CCOO)]$ group is not as electron withdrawing as the $[CF_3COO]$ group but more so than the $[CH_3COO]$ group consistent with our earlier conclusions [5]. Note that the Cr–O distances for the $[CF_3COO]$ ligand are significantly longer than those for the cluster carboxylate ligand, e.g., Cr(1)–O(3)=2.028(4) Å, Cr(1)–O(1)=1.993(4) Å.

3.1.2. $Sm_2\{\mu\text{-}OOCCCo_3(CO)_9\}_2\{\mu\text{-}OOCCF_3\}_4\{(CO)_9Co_3CCOOH\}_2(THF)_2\cdot 2THF$, **2**

The structure of **2**, which is shown in Fig. 2 (Table 3) and Fig. 8b, exhibits a dimeric Sm(III) core (Sm–Sm= 4.239 Å) asymmetrically bridged by four $[CF_3COO]^-$

ligands. Two $[CF_3COO]^-$ ligands apparently chelate one Sm(III) each and are positioned such that one oxygen atom each also bridges the two Sm atoms. Additionally, each Sm(III) center is chelated by one $[(CO)_9Co_3CCOO]^-$ ligand plus coordinated to one THF molecule and one $(CO)_9Co_3CCOOH$ cluster acid which also forms a hydrogen bond to an oxygen atom of the chelating cluster ligand. Thus, the core is closely related to that found in the $[Sm_2\{OOCCH_3\}_3\{H_2O\}_2]_2$ dimer, i.e. CF_3COO^- is replaced by acetate, the cluster ligand by acetate and the THF and the cluster acid by two H_2O molecules [27]. As far as the coordinated cluster ligands are concerned, they form a linear array in the same manner as compound **1** but with a substantially larger distance separating them.

3.2. Cluster coordination number=3

3.2.1. $PtCo\{\mu\text{-}OOCCCo_3(CO)_9\}_3(\mu\text{-}OOCCH_3)\{(CO)_9Co_3CCOOH\}$, 3

The structure of **3**, shown in Fig. 3 (Table 4) and Fig. 8c, exhibits a Co(II)Pt(II) core bridged by three cluster carboxylates and one acetate. The P(II) center is in a square planar environment of oxygen atoms; however, the Pt–Co distance is well within the sum of the metal covalent radii (Pt–Co(1)=2.506(1) Å). The Co(II) center is axially coordinated by the oxygen of a cluster acid the presence of which is corroborated by the IR spectrum in that a band at 1642 cm^{-1} characteristic of the acid is observed [28]. As is common with coordinated cluster acids, the OH group is also hydrogen bonded to one of the oxygen atoms of a bridging cluster ligand. Thus, the Co(II) center may be considered either five or six coordinate depending how the Pt atom is viewed. The three coordinated tricobalt clusters form a T-shaped or isosceles triangular array.

3.2.2. $ZnCo\{\mu\text{-}OOCCCo_3(CO)_9\}_3\{Co(CO)_4\}\{2\text{-}(CH_3)C_4H_7O\}$, 4

The structure of cluster **4**, shown in Figs. 4 and 8d, consists of a Zn(II)Co(II) nonbonded dimer bridged by three cluster carboxylates. Consequently, the three cluster ligands display a trigonal arrangement. The two metal cations have tetrahedral environments: the fourth position being occupied with methyl THF in the case of Zn and a $[Co(CO)_4]^-$ fragment in the case of Co. The methyl group of the THF ligand is oriented towards the center of the cluster and lies between two of the cluster ligands.

The Co(1)–Co(11) distance of 2.419 (4) Å (Table 5) is close to that found in a $Co_3(CO)_9(\mu_3\text{-}CR)$ cluster (i.e. 2.450(4) Å) and consistent with an unsupported metal–metal bond. Of course, one cannot determine from structural data whether $[Co(CO)_4]^-$ or $Co(CO)_4$ is bound to the cobalt center. Therefore, it is not at all clear how one should view the formal oxidation state of the Co atom in the ZnCo core. ^1H NMR signals for the coordinated methyl THF can be observed for **4** in CD_2Cl_2 with somewhat larger than normal chemical shifts. The IR spectrum distinctly shows the signature [28] of bridging carboxylates consistent with the solid state structure. In addition, the bands observed at 1984–1944 cm^{-1}, not present in the other compounds, are assigned to the $Co(CO)_4^-$ moiety. The band position suggests considerably more negative charge than present on the $Co(CO)_3$ groups of the ligand clusters which is consistent with a polar (donor–acceptor) Co(1) – Co(11) metal–metal bond. Thus, we view Co(11) as a Co(II) center.

3.3. Cluster coordination number=4

3.3.1. $CoCr_2(\mu_3\text{-}O)\{\mu\text{-}OOCCCo_3(CO)_9\}_4(\mu\text{-}OOCCH_3)_2\{(CO)_9Co_3CCOOH\}_2(H_2O)\cdot C_7H_8$, 5a; $Cr_3(\mu_3\text{-}O)\{\mu\text{-}OOCCCo_3(CO)_9\}_4(\mu\text{-}OOCCH_3)_2\{(CO)_9Co_3CCOOH\}(CH_3OOH)_2\cdot C_7H_8$, 5b

Compounds **5** are related to the known organic carboxylates of the type $Cr_3(\mu_3\text{-}O)(\mu\text{-}OOCR)_7(L)_3$ [29], e.g. $Cr_3(\mu_3\text{-}O)\{\mu\text{-}OOCR\}_6(py)_3$, a mixed valence trimer with one Cr(II) and two Cr(III) centers [30], which have been extensively studied [31,32]. Because of the kinetic inertness of the Cr(III) centers, a simple cluster carboxylate exchange strategy does not lead to the cluster analogs. However, partially "exchanged" analogs were obtained from the dimeric Cr(II) cluster carboxylate; namely both mixed metal **5a** and homonuclear **5b** complexes. Mixed metal species such as $Cr_2Co(\mu_3\text{-}O)\{\mu\text{-}OOCCMe_3\}_6(H_2O)_3$ [33] have also been studied previously [34].

The structure of **5a** is shown in Figs. 5 and 8e (Table 6) and the core structure is similar to that of a $Cr_2Co(\mu_3\text{-}O)(\mu\text{-}OOCR)_6$ complex described earlier [33]. Both Cr(III) and Co(II) centers are octahedral. The existence of cluster acid connected to each to the Cr centers is evident from the IR band at 1695 cm^{-1} which is typical of a carboxylic acid. The structure of the cluster **5b** is shown in Fig. 6. Oxo-trimers of Cr_3(III, III, III) have been reported much more frequently [29] than Cr_3(II, III, III) compounds [30]. The EPR signal observed for **5b** is consistent with that exhibited by $Cr_3(\mu_3\text{-}O)(\mu\text{-}OOCCH_3)_7$ [35]. Thus, the fact that **5a** is EPR silent is ascribed to the presence of the octahedral Co(II) d^7 metal ion.

3.4. Cluster coordination number=5

3.4.1. $[C_{10}H_6(N(CH_3)_2)_2H][Co_2\{\mu\text{-}OOCCCo_3(CO)_9\}_3\{OOCCCo_3(CO)_9\}_2]$, 6

Two species are found in the solid state: a $[C_{10}H_6(N(CH_3)_2)_2H]^+$ cation and the anionic cluster coordination compound shown in Figs. 7 and 8f (Table 7). Reminiscent of **4**, **6** contains a Co(II)Co(II) non-bonded (3.502(2) and 3.431(2) Å in the two independent anions) dimetal core bridged by three cluster carboxylate ligands. The Co(II) centers have tetrahedral environments but, in

contrast to **4**, the remaining position in each is filled by a monodentate cluster ligand. The net result is a trigonal bipyramidal array of coordinated cluster ligands.

Consistent with the nonbonded tetrahedral Co(II) centers, compound **6** is paramagnetic and displays an EPR signal both in the solid state and in a frozen glass at low temperature. The IR spectrum distinctly shows the signatures [28] of both bridging and monodentate carboxylates consistent with the solid state structure. The electronic spectrum is similar to that of the cluster ligand but the position of the main band is shifted 15 nm to the red compared to the free cluster acid.

4. Conclusions

Due to the instability of a cluster carboxylate salt such as $Na[(CO)_9Co(\mu_3\text{-}CCOO)]$ towards cluster degradation, simple metathesis chemistry cannot be used to form the desired coordination compounds. In past work we have shown that the protolysis of group 12 metal alkyls provides one route to cluster carboxylates and cluster ligand exchange reactions with M(II) metal acetates provides another. This work provides additional examples of the metal acetate exchange route and also establishes new synthetic pathways to cluster carboxylates. Some are analogs of known organic carboxylates whereas others exhibit unusual features that reflect the unique properties of the tricobalt cluster substituent.

Extension of the normal acetate exchange pathway to Pt has led to the characterization of **2** with an unusual Pt–Co core. When applied to metal trifluoroacetates, the ligand exchange pathway permits the isolation of a M_2L_4 dimer carboxylate, **1**, with two trans cluster ligands. Thus, we now have a set of M_2L_4 compounds with two, three, and four cluster ligands [10,12,21] In addition, this route provides an example of a samarium cluster metal carboxylate, **2**.

To avoid the use of reagents like $ZnEt_2$, we examined the reaction of M(II) hydroxides. In the case of Zn(II), reaction in THF cleanly provides the desired $Zn_4(m_4\text{-}O)\{\mu\text{-}OOC\text{-}CCo_3(CO)_9\}_6$ [5]. Use of a substituted THF leads to the isolation of **4** in which an active Zn fragment is trapped by Co(II) and $[Co(CO)_4]^-$ produced by concurrent degradation of the tricobalt cluster [14].

The redox properties of the tricobalt cluster provide a route from $Cr(II)_2L_4$ complexes to oxo-trimers with $Cr(III)_2$ plus Co(II), **5a**, or Cr(II), **5b**, cores. Solvent is the key as use of a coordinating solvent like THF leads to simple ligand exchange [36].

Finally, although treatment of $(CO)_9Co(\mu_3\text{-}CCOOH)$ with strong base leads to ready decomposition, the use of a bulky organic base provides a salt that is considerably more stable. Presumably, in the tight ion pair the nucleophilic carboxylate functionality is shielded by the cation. Inhibition of decomposition permits the isolation of the first anionic cluster metal carboxylate, **6**.

We have shown previously that cluster metal carboxylates serve as precursors for heterogeneous catalysts for hydrogenation reactions. These catalysts possess promising activities and selectivities for demanding reactions such as the hydrogenation of crotonaldehyde to the unsaturated alcohol [11]. Most importantly we have shown that not only do catalytic properties depend on metal core composition but also on the geometry of the cluster array in the catalyst precursor, e.g. $Co_4(\mu_4\text{-}O)\{\mu\text{-}OOC\text{-}CCo_3(CO)_9\}_6$ imparts very different properties to the catalyst than those generated by $Co_2\{\mu\text{-}OOC\text{-}CCo_3(CO)_9\}_4$. Hence, the compounds illustrated in Fig. 8 provide a library of cluster arrays that can be used to further change, and hopefully refine, the properties of the catalysts derived from them.

Supplementary data

Positional parameters and estimated equivalent isotropic thermal parameters, anisotropic thermal parameters, full list of atomic distances and angles are available from the Cambridge Crystallographic Data Centre, 12 Union Road, Cambridge CB2 1EZ, UK.

Acknowledgements

We are grateful for the support of the National Science Foundation. VCP also thanks the Department for a Reilly Fellowship.

References

[1] M.J. Irwin, G. Jia, N.C. Payne, R.J. Puddephatt, Organometallics 15 (1996) 51.
[2] J.R. Bleeke, R. Behm, A.M. Beatty, Organometallics 16 (1997) 1103.
[3] Y.G. Aronoff, B. Chen, G. Lu, C. Seto, J. Schwartz, S.L. Bernasek, J. Am. Chem. Soc. 119 (1997) 259.
[4] S. Achar, J.J. Vittal, R.J. Puddephatt, Organometallics 15 (1996) 43.
[5] W. Cen, K.J. Haller, T.P. Fehlner, Inorg. Chem. 32 (1993) 995.
[6] M.R. Jordan, P.S. White, C.K. Schauer, M.A. Mosley III, J. Am. Chem. Soc. 117 (1995) 5403.
[7] D.L. Sunick, P.S. White, C.K. Schauer, Organometallics 12 (1993) 245.
[8] X. Lei, M. Shang, T.P. Fehlner, Organometallics 16 (1997) 5289.
[9] M.A. Bañares, L. Dauphin, V. Calvo-Perez, T.P. Fehlner, E.E. Wolf, J. Catal. 152 (1995) 396.
[10] M.A. Bañares, L. Dauphin, X. Lei, W. Cen, M. Shang, E.E. Wolf, T.P. Fehlner, Chem. Mater. 7 (1995) 553.
[11] M. Bañares, A.N. Patil, T.P. Fehlner, E.E. Wolf, Catal. Lett. 34 (1995) 251.
[12] W. Cen, P. Lindenfeld, T.P. Fehlner, J. Am. Chem. Soc. 114 (1992) 5451.
[13] W. Cen, K.J. Haller, T.P. Fehlner, Inorg. Chem. 30 (1991) 3120.
[14] W. Cen, K.J. Haller, T.P. Fehlner, Organometallics 11 (1992) 3499.
[15] W. Cen, Ph.D thesis, University of Notre Dame, 1992.

[16] V. Calvo-Perez, Ph.D. thesis, University of Notre Dame, 1995.
[17] V. Calvo-Perez, T.P. Fehlner, A.L. Rheingold, Inorg. Chem. 35 (1996) 7289.
[18] X. Lei, M. Shang, A. Patil, E.E. Wolf, T.P. Fehlner, Inorg. Chem. 35 (1996) 3217.
[19] X. Lei, M. Shang, T.P. Fehlner, Organometallics 15 (1996) 3779.
[20] H. Shimomura, X. Lei, M. Shang, T.P. Fehlner, Organometallics 16 (1997) 5302.
[21] X. Lei, M. Shang, T.P. Fehlner, R. Werner, W. Haase, D. Hautot, G.J. Long, J. Organomet. Chem. 541 (1997) 57.
[22] C.J. Bilgrien, R.S. Drago, C.J. O'Connor, N. Wong, Inorg. Chem. 27 (1988) 1410.
[23] T. Yamaguchi, N. Nishimura, T. Ito, J. Am. Chem. Soc. 115 (1993) 1612.
[24] M.R. Hatfield, Inorg. Synth. 3 (1966) 148.
[25] F.A. Cotton, W.H. Ilsey, W. Kaim, J. Am. Chem. Soc. 102 (1980) 3473.
[26] F.A. Cotton, G.W. Rice, Inorg. Chem. 17 (1978) 2004.
[27] A. Lossin, G. Meyer, R. Fuchs, J. Strahle, Z. Naturforsch. 47 (1992) 179.
[28] R.C. Mehrotra, R. Bohra, Metal Carboxylates, Academic Press, New York: 1983.
[29] J.E. Bradshaw, D.A. Grossie, D.F. Mullica, D.E. Pennington, Inorg. Chim. Acta 141 (1988) 41.
[30] F.A. Cotton, W. Wang, Inorg. Chem. 21 (1982) 2675.
[31] C. Janiak, J. Silvestre, K.H. Theopold, Chem. Ber. A 126 (1993) 631.
[32] C.E. Anson, N. Chai-Sa'ard, J.P. Bourke, R.D. Cannon, U.A. Jayasooriya, A.K. Powell, Inorg. Chem. 33 (1993) 1502.
[33] A.S. Batsanov, G.A. Timko, Y.T. Struchkov, N.V. Gerbeleu, O.S. Manole, Koord. Kim. 17 (1992) 922.
[34] R.D. Cannon, U.A. Jayassooriya, L. Montri, A.K. Saad, E. Karu, S.K. Bollem, W.R. Sanderson, A.K. Powell, A.B. Blake, J. Chem. Soc. Dalton Trans. (1993) 2005.
[35] M.K. Nagi, A. Harton, S. Donald, Y.-S. Lee, M. Sabat, C.J. O'Connor, J.B. Vincent, Inorg. Chem. 34 (1995) 3813.
[36] T.P. Fehlner, V. Calvo-Perez, W. Cen, J. Electron Spectr. 66 (1993) 29.